ELSEVIER

Earth and Planetary Science Letters 154 (1998) 221–235

EPSL

Depleted spinel harzburgite xenoliths in Tertiary dykes from East Greenland: Restites from high degree melting

Stefan Bernstein [a,*], Peter B. Kelemen [b,1], C. Kent Brooks [a,c,2]

[a] *Danish Lithosphere Centre, Øster Voldgade 10, DK-1350 Copenhagen K, Denmark*
[b] *Woods Hole Oceanographic Institution, Woods Hole, City, MA 02543, USA*
[c] *Geological Institute, University of Copenhagen, Øster Voldgade 10, DK-1350 Copenhagen K, Denmark*

Received 28 April 1997; revised 19 September 1997; accepted 4 October 1997

Abstract

A new collection of mantle xenoliths in Tertiary dykes from the Wiedemann Fjord area in Southeast Greenland shows that this part of the central Greenland craton is underlain by highly depleted peridotites. The samples are mostly spinel harzburgites with highly forsteritic olivines (Fo_{87-94}, average $Fo_{92.7}$). This, together with unusually high modal olivine contents (70–>95%), places the Wiedemann harzburgites in a unique compositional field. Relative to depleted Kaapvaal harzburgites with comparable Fo in olivine, the Wiedemann samples have considerably lower bulk SiO_2 (average 42.6 wt% versus 44–49 wt%). Spinel compositions are similar to those in other sub-cratonic harzburgites. Pyroxene equilibrium temperatures average 850°C, which is above an Archaean cratonic geotherm at an inferred pressure of 1–2 GPa, but low enough so that it is unlikely that the xenoliths represent residual peridotites created during Tertiary magmatism. Among mantle samples, the Wiedemann harzburgites are, in terms of their bulk composition, most similar to harzburgites from the ophiolites of Papua New Guinea (PNG) and New Caledonia (NC). One hypothesis is that the Wiedemann harzburgites, along with PNG and NC harzburgites, formed via dissolution of pyroxene from previously depleted peridotites, possibly beneath a volcanic arc. If so, higher spinel Cr/Al in Wiedemann samples may reflect a deeper origin compared to PNG and NC peridotites. Alternatively, using proposed primitive mantle compositions as a protolith, the Wiedemann harzburgites can be modeled as the residue after extraction of some 40% melt. The composition of this calculated hypothetical melt in terms of CaO, Al_2O_3, FeO, MgO and SiO_2 is similar to published experimental data on high degree melts of peridotite at 2–3 GPa. Munro-type komatiites lie close to these calculated and experimental melts but are slightly displaced towards low degree experimental melts at higher pressure (e.g., 6 GPa). We conclude that the Wiedemann harzburgites formed as a residue after about 40% melting, and that they may represent shallow, refractory residues after polybaric melting initiated at pressures ≥ 7 GPa and continuing to relatively low pressures (2–3 GPa or less). Extraction and aggregation of polybaric melts would produce liquids similar to Munro-type komatiites. © 1998 Elsevier Science B.V.

Keywords: harzburgite; xenoliths; Greenland; partial melting; komatiite

1. Introduction

The highly refractory nature of mantle xenoliths from beneath the Archaean Kaapvaal craton, South

* Corresponding author. Tel.: +45 3814 2656. Fax: +45 3311 0878. E-mail: sb@dlc.ku.dk
Tel.: 508 457 2000, ext. 2956. E-mail: peterk@cliff.whoi.edu
Tel.: 45 3532 2417. E-mail: kentb@geo.geol.ku.dk

PII S0012-821X(97)00175-1

Africa, was realized in the early 1970s (e.g. [1]). Since then, several authors have demonstrated that mantle xenoliths from Archaean cratons, compared to those from Proterozoic and Phanerozoic crustal terrains, in general have higher modal olivine, forsterite content (Fo = Mg# = atomic Mg/(Mg + Fe)∗100) in olivine (often $> Fo_{91}$), and Cr/(Cr + Al) in spinels [2–4]. These characteristics have been explained in terms of extensive melt extraction from the mantle, leaving a residue highly depleted in basaltic components (e.g. [2,3,5–7]). Further, because of the high degrees of melting inferred, the refractory mantle material has been linked to the extraction of komatiites in the Archaean [8]. Here we present the mineral chemistry of a new suite of spinel peridotite xenoliths of mantle origin that may help to shed light on the connection between depleted lithospheric mantle and komatiites.

2. Occurrence and nature of the Wiedemann Fjord xenoliths

Mantle peridotite xenoliths in East Greenland were found in erratic blocks by Brooks and Rucklidge [9], and their refractory nature was established by the olivine-rich modal composition and highly forsteritic olivine ($Fo_{92.5}$). Wiedemann Fjord was visited again in the summer of 1995 and two main localities of xenolith-bearing dykes were discovered (Fig. 1). The dykes intrude Tertiary plateau basalts [10], which were extruded between 58 and 56 Ma [11,12] and reach a thickness in excess of 6 km [13]. The main basaltic volcanism terminated at about 47 Ma [14]. To the southwest, the basalts rest on gneissic basement with model ages between 3.02 and 2.79 Ga (Sm–Nd) and between 3.07 and 2.51 Ga (Pb–Pb) [15]. Further to the northeast, the area was affected

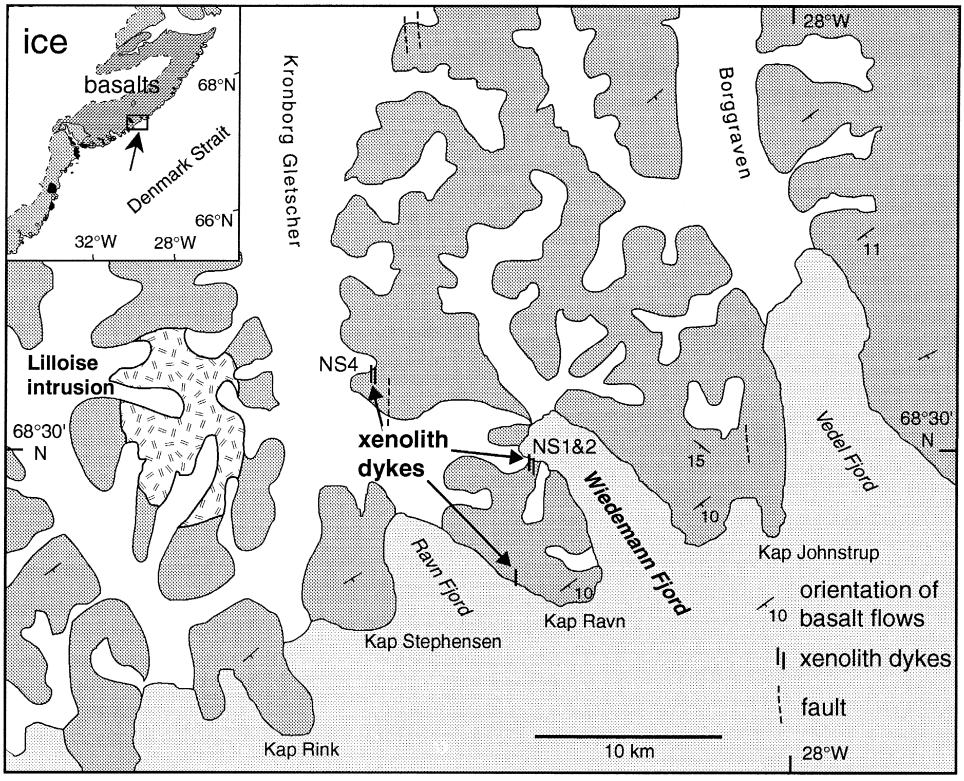

Fig. 1. The xenolith-bearing dykes with the two main xenolith localities (NS1 and 2 and NS4). The dykes run N–S and are vertical (thick black lines). Dark gray = basalts of the Geikie Plateau Formation basalts. Stippled body is the 49 my ultramafic–mafic Lilloise intrusion. Insert gives the location of the larger map.

by Caledonian thrusts and granitic intrusions [16]. The basement is not exposed around Wiedemann Fjord, and it is unknown whether it is Archaean or Caledonian.

The xenolith-bearing dykes are 40.48 ± 0.27 Ma (Ar–Ar method; R. Duncan, pers. commun.), post-dating both continental break-up, by roughly 15 Ma, and the last important magmatic episode, by 9–6 Ma. The dyke location and their N–S strike and vertical dip correlate with a N–S zone of prominent faulting [13] (Fig. 1).

The xenolith-bearing dykes are 0.2–1.5 m wide and occur in clusters of less than 5. They commonly have a distinct yellowish alteration halo (2–15 cm wide), consisting of calcite and clay minerals. The dykes themselves weather to a dark brown colour. Subhedral, kaersutitic amphibole makes up about 50% of the matrix of the rock, in addition to 10% euhedral, microphenocrysts of clinopyroxene, which is zoned from colourless cores to deep lilac-coloured rims. Other rare, large crystals include olivine, orthopyroxene and chrome-spinel, interpreted as mantle xenocrysts [9]. The mesostasis in the dykes consists largely of plagioclase and alkali feldspar. Small titanomagnetite grains are distributed throughout the rock. The whole rock chemistry is that of an alkali basalt (Table 1).

Xenoliths occur in a central plane parallel to dyke margins. The xenoliths have crudely discoidal shapes, with large aspect ratios. They range in size from 2–3 mm to 6 cm in maximum dimension, with an average of about 1–2 cm. In general, they are fresh but in 2–3%, all olivine and orthopyroxene is replaced by serpentine. About 50% of the xenoliths show 1–2 mm alteration rims where again olivine and orthopyroxene are replaced. The rest show little hydrothermal alteration. Invasion of melt from the host is only observed in few xenoliths. In some xenoliths, orthopyroxene have reaction rims (1–2 mm wide, fine-grained) against the host dyke. Partial melting of the xenoliths, probably during heating and decompression during ascent in the dykes, is indicated by

Table 1
Compositions of average Wiedemann harzburgite; estimated primitive mantle; computed liquid in equilibrium with average Wiedemann harzburgite; experimental melts, their starting material; and the matrix of the nodule-bearing dyke

		SiO_2	TiO_2	Al_2O_3	FeO*	MnO	MgO	CaO	Na_2O	Sum	Mg#	Ol–Fo
Average Wiedemann harzburgite		42.63	0.01	0.82	6.65	0.19	48.43	0.19	0.03	98.95		
HZPUM	primitive mantle	45.96	0.18	4.06	7.54	0.13	37.78	3.21	0.33	99.19		
Pyrolite	primitive mantle	45.10	0.20	3.30	8.00	0.15	38.10	3.10	0.04	97.99		
38% melt of HZPUM	(computed liquid)	51.39	0.46	9.34	9.00	0.03	20.40	8.15	0.86	99.63	81.78	93.54
40% melt of pyrolite	(computed liquid)	48.81	0.49	7.02	10.03	0.01	22.60	7.47	0.96	97.39	81.69	93.50
	P (kbar)											
Kettle River	start material	44.90	0.15	4.26	8.02	0.13	37.30	3.45	0.22	98.43		
36% melting	30	48.98	0.48	11.06	9.45		19.71	8.78	0.77	99.23	80.50	93.02
52% melting	30	47.96	0.39	9.50	9.19		23.89	7.70	0.52	99.15	83.73	94.32
11% melting	60	44.97	1.01	6.37	12.64		23.26	9.05	0.80	98.10	78.46	92.16
HW	start material	45.20	0.71	3.54	8.47	0.14	37.50	3.08	0.57	99.21		
	20	50.18	1.74	8.61	9.34	0.90	19.96	7.40	1.40	99.53	79.20	92.47
	20	49.16	1.40	6.83	9.19	0.15	24.96	6.11	1.13	98.93	82.87	93.98
	30	47.79	1.81	8.55	9.55		21.39	7.60	1.52	98.21	79.96	92.79
TQ	start material	44.95	0.08	3.22	7.60	0.14	40.03	2.99	0.18	99.19		
	20	49.21	0.25	9.58	8.61		21.40	9.04	0.57	98.66	81.58	93.46
	20	49.28	0.36	9.94	9.08		20.57	9.54	0.47	99.24	80.14	92.87
	30	48.46	0.22	8.62	8.88		23.85	8.13	0.51	98.67	82.71	93.92

Nodule-bearing dyke (chill):	SiO_2	TiO_2	Al_2O_3	FeO	MnO	MgO	CaO	Na_2O	K_2O	P_2O_5	H_2O	Sum
#GGU429285	41.34	3.51	13.03	11.70	0.17	9.84	10.94	1.91	2.02	0.79	3.43	98.68

HZPUM is Hart and Zindlers primitive upper mantle [43]; pyrolite is from Ringwood [42]. Experiments on Kettle River peridotite: [45]; HW (Hawaiian pyrolite) and TQ (Tinaquillo Iherzolite): [49].

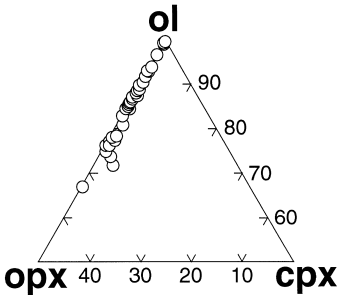

Fig. 2. Modal composition in terms of the main silicate phases, olivine (ol), orthopyroxene (opx), and clinopyroxene (cpx), as determined by point counting (table 1, **EPSL Online Background Dataset**).

10 μm scale zones of fine-grained (~1 μm) clinopyroxene, olivine, and other, unidentified silicate phases around clinopyroxene.

A suite of 90 xenoliths forms the basis of this study. All are peridotites, consisting of olivine, orthopyroxene, Cr–Al spinel and Ca-rich clinopyroxene in varying proportions. Only 7 were found to contain traces (less than 1 vol%) of additional phases, 2 with phlogopite and 5 with amphibole. More than 80% of the xenoliths are equant and tabular granoblastic, the remainder being porphyroclastic (15%) and coarse (5%), using the nomenclature of Harte [17]. One harzburgite xenolith with high (33 vol%) modal orthopyroxene has igneous (cumulate) texture. The grain size is typically 0.1–5 mm (granoblastic); 0.1–3 mm (porphyroclastic) and 2–6 mm (coarse). Olivine crystals often have undulose or lamellar extinction, especially in larger grains (> 1 mm).

Modal composition of 46 xenoliths was determined by point counting of thin sections (table 1, **EPSL Online Background Dataset** [3]). The uncertainty in olivine and orthopyroxene proportions estimated in this way is typically ±4% [18]. Results are shown in Fig. 2. Most xenoliths are harzburgites, and some can be classified as dunites (< 10 vol% pyroxene). Spinel typically comprises about 1 vol% of all samples (ranging from 0.2 to 4 vol%). It is uncertain whether the dunite samples represent larger dunite domains or inhomogeneities larger than the dunite xenoliths. Harzburgites and dunites with more than 85% olivine have less than 1% clinopyroxene.

3. Analytical data

3.1. Mineral chemistry

Minerals in 90 xenoliths were analysed by electron microprobe. Accelerating voltage was 15 kV, beam current about 15 nA and beam diameter about 2 μm. Mg, Si, Ti, Mn, and Fe were measured by energy dispersive spectroscopy (140 s counting time). Na, K, Al, Ca, Ni, and Cr were measured by wavelength dispersive spectroscopy, with 40 s counting time on peaks and 20 s on background, except for Na and K, which were counted for 20 s on peaks and 10 s on background. Analyses were corrected for drift by linear interpolation between blocks of standard analyses. These corrections were minor, typically ~1% relative. Results are presented in tables 2–4 (**EPSL Online Background Dataset** [4]), where the composition tabulated for each sample is the average of the number of analyses listed. The main features are described below:

Olivine crystals are unzoned. Variation in Fo within a single xenolith is typically less than ±0.2% (abs). Over the entire suite of samples, olivine ranges from $Fo_{87.6}$ to $Fo_{94.0}$. Most xenoliths have $> Fo_{92.0}$ (74%; Fig. 3). The xenolith with igneous (cumulus) texture has low Fo (< 90.7), and some xenoliths with metamorphic texture also have low Fo values. Nickel in olivine ranges from 1870 to 3350 ppm (0.240–0.425 wt% NiO). Samples with olivine between Fo_{90} and Fo_{94} have Ni between 2400 and 3350 ppm, and show no correlation between Fo and Ni. Two samples with Fo around 88 define the lower end of the Ni compositional range.

Orthopyroxene is present in all but a few xenoliths. It mostly occurs as interstitial grains with an average grain size smaller than that of olivine, or, less often, as larger grains with grain size greater than or equal to that of olivine. The Kd for Fe–Mg exchange between olivine and orthopyroxene (molar Fe/Mg in olivine/Fe/Mg in orthopyroxene) falls in the range 1.010 and 1.125 for all samples. This is similar to the experimentally determined Kd, which ranges from 1.03 to 1.18 for 1.0–2.5 GPa and 700–1100°C [19]. Within-sample variation and intra-crys-

[3] URL: http://www.elsevier.nl/locate/epsl, mirror site: http://www.elsevier.com/locate epsl.

[4] URL: http://www.elsevier.nl/locate/epsl, mirror site: http://www.elsevier.com/locate epsl.

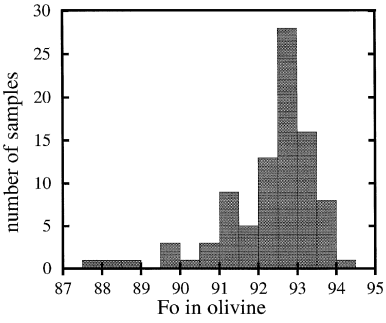

Fig. 3. Forsterite content in olivine from individual xenoliths. N(samples) = 90. The composition of olivine in each sample is an average of 3–15 analyses.

talline zoning in orthopyroxene are not observed in any of the xenoliths. In the entire sample suite, Al_2O_3 and CaO vary from 0.78 to 4.22 wt% and from 0.12 to 1.26 wt%, respectively. CaO correlates poorly with Mg#, whereas Al_2O_3 shows a good negative correlation with Mg#. Cr_2O_3 varies between 0.14 and 0.72 wt%.

Clinopyroxene has been found in 31 out of the 90 xenoliths. Where present, it generally comprises less than 1 vol%. Size is at the low end of the total grain size range as reported in table 1 (**EPSL Online Background Dataset** [5]). The calculated Kd for Fe/Mg exchange between olivine and clinopyroxene or between ortho- and clinopyroxene varies greatly: 1.11–1.86 and 1.02–1.90, respectively. For 1.0–2.5 GPa and 700–1100°C, experimental Fe/Mg Kd values span 1.04–1.91 (clinopyroxene/olivine) and 1.01–1.65 (clinopyroxene/orthopyroxene) [19]. The range of measured Kd values for our samples, although large, is therefore within the range of experimentally determined values. Clinopyroxene also shows a considerable variation in Na_2O (0.28–2.01 wt%); Al_2O_3 (1.11–6.76 wt%); TiO_2 (0.01–0.73 wt%) and Cr_2O_3 (0.38–1.08 wt%). Again it should be stressed that this is inter-sample variation because no significant variation within individual samples was detected.

Spinel is present in all but 5 samples. Individual grains are homogeneous down to the resolution of the electron microprobe. Crystals often have an elon-

[5] URL: http://www.elsevier.nl/locate/epsl, mirror site: http://www.elsevier.com/locate epsl.

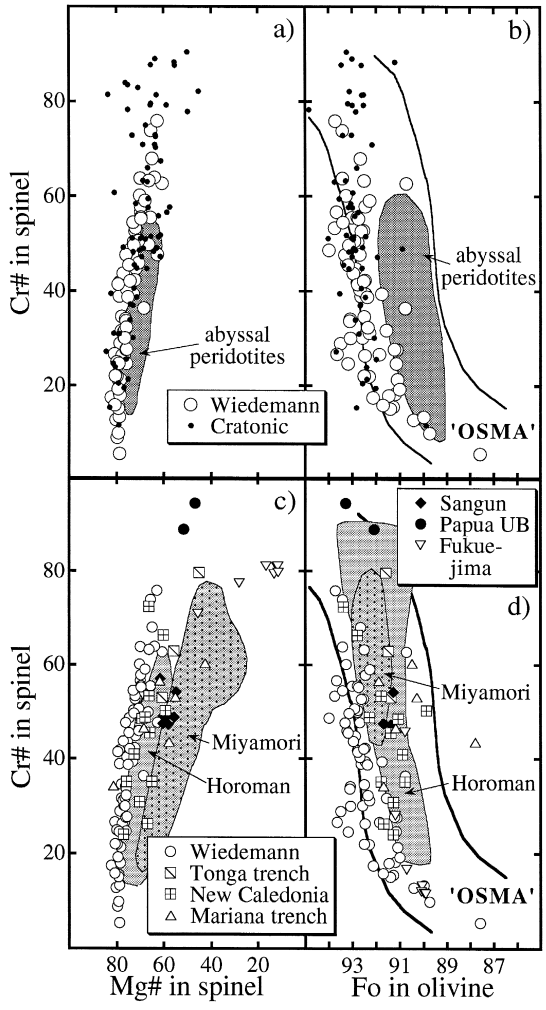

Fig. 4. Compositional variation within all Wiedemann Fjord xenoliths. (a) Spinel compared to that of spinel from abyssal peridotites [33], and from cratonic spinel peridotite xenoliths ([71–75], and Boyd, pers. commun.). (b) Comparison between coexisting spinel and olivine with the field of abyssal peridotites and data from cratonic spinel peridotites (references as above). The Olivine–Spinel–Mantle Array (OSMA) is from Arai [20]. Note that the field defined by the Wiedemann xenoliths in both figures is displaced to the left relative to abyssal peridotites (i.e. higher Mg# in spinel and olivine for a given Cr# in spinel) but the Wiedemann harzburgites are indistinguishable from the subcratonic spinel peridotites. (c) and (d) Present compositional data of spinel and spinel–olivine pairs from arc settings (Horoman, Japan: [76,77]; Miyamori, Japan: [78,79]; Fukue-jima, Japan: [80]; Sangun-Yamaguchi, Japan: [81]; Papuan Ultramafic Belt: [82]; New Caledonia: [83]; Tonga trench: [84]; Mariana trench: [85]).

gated outline. Within-sample compositional variation is not observed. Variation in Cr# (molar Cr/(Cr + Al) × 100%) is from 5.44 to 75.87. Mg# correlates negatively with Cr#, and varies from 82.51 to 60.75 (Fig. 4a). NiO varies from 0.44 wt% to 0.05 wt% and correlates negatively with Cr#. Further, there is a good positive correlation between Fo in olivine and Cr# in spinel for coexisting olivine–spinel pairs, as demonstrated in Fig. 4b. Compared to abyssal peridotites, the Wiedemann spinels are displaced towards higher Mg#, and also extend to higher Cr# (Fig. 4a). Similarly the Wiedemann xenoliths fall along the high Fo edge of the 'OSMA' = ''olivine–spinel mantle array'', as defined by Arai [20] (Fig. 4b).

3.2. Whole-rock composition

Whole-rock composition was calculated using the modal composition obtained by point counting (table 1, **EPSL Online Background Dataset** [6]). The calculation used a least-square fit with average mineral analyses having appropriate Mg# and Cr#. The errors in this method mainly stem from errors in estimating the modal composition of the xenoliths. Because of the high proportions of olivine to the other phases, the errors in calculated SiO_2, MgO, FeO and NiO will be small, relative to the errors in, for example, calculated CaO that is dependent on the uncertain modal proportion of clinopyroxene. Average xenolith composition is presented in Table 1.

4. Geothermometry

Equilibrium temperatures were calculated on the basis of the mineral data in tables 3 and 4 (**EPSL Online Background Dataset** [7]). Two geothermometers give realistic temperature estimates over a range of compositions in mantle xenoliths. These are: Ca in orthopyroxene ($T_{Ca\text{-}in\text{-}opx}$; [19]); and Al–Cr exchange between orthopyroxene and spinel (T_{Al-Cr}; [21]). $T_{Ca\text{-}in\text{-}opx}$ is based on equilibrium between orthopyroxene and clinopyroxene. For our samples, use of this thermometer is problematic since clinopyroxene is scarce or absent in many samples. Further, $T_{Ca\text{-}in\text{-}opx}$ includes the pressure dependent exchange of Ca between pyroxenes, so that a pressure needs to be chosen. In the present case, a pressure of 1.5 GPa was used. Increasing the pressure to, for example, 2.0 GPa will result in an average increase in $T_{Ca\text{-}in\text{-}opx}$ of about 20°C. In the Al–Cr exchange thermometer (T_{Al-Cr}), the required coexistence of spinel and orthopyroxene together is observed in almost all of our samples. The results of the calculations are shown in table 1 (**EPSL Online Background Dataset** [8]) and Fig. 5. The common temperature interval is 780–900°C, and about 70% of the measured samples have $\Delta(T_{Ca\text{-}in\text{-}opx}) - (T_{Al-Cr}) < 25$°C. A few of the outliers in Fig. 5 have Cr and Al in orthopyroxene that is close to the limits for the range where the T_{Al-Cr} is defined.

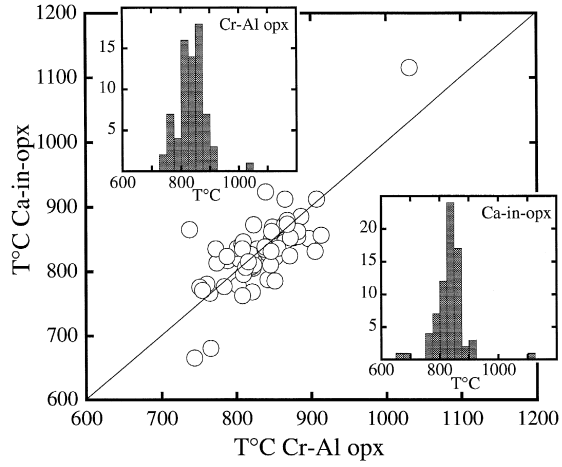

Fig. 5. Equilibrium temperatures determined on the basis of orthopyroxene chemistry (see text). The T_{Cr-Al} is independent of pressure, while a pressure of 1.5 GPa has been assumed for the $T_{Ca\text{-}in\text{-}opx}$. Both thermometers give an average temperature of about 850°C (see insert histograms).

The close correlation between these two thermometers suggests that the estimated pressure of 1.5 GPa is close to the equilibrium pressure for the majority of the xenoliths. Temperatures lack correlation with texture and chemistry, the exception being sample 2-24Ab. It has an igneous texture and the highest calculated temperature of 1030–1116°C. Finally, the rough agreement between orthopyroxene–

[6] URL: http://www.elsevier.nl/locate/epsl, mirror site: http://www.elsevier.com/locate epsl.

[7] URL: http://www.elsevier.nl/locate/epsl, mirror site: http://www.elsevier.com/locate epsl.

[8] URL: http://www.elsevier.nl/locate/epsl, mirror site: http://www.elsevier.com/locate epsl.

spinel and orthopyroxene–clinopyroxene thermometry suggests that all three phases approached equilibrium at temperatures close to 850°C.

5. Discussion

We will first discuss how the temperatures recorded by the Wiedemann harzburgite xenoliths constrain their age and thermal evolution. Second, we compare the Wiedemann xenolith compositions to other peridotites worldwide, and investigate possible geological settings for their formation. Finally, we present hypotheses for their origin as products of melt/rock reaction in the upper mantle or as residues from high degree partial melting, and their possible relationship to the generation of certain types of komatiites.

5.1. Constraints on the origin and thermal evolution of the East Greenland lithospheric mantle

Given the absence of plagioclase and garnet from the xenoliths, even those containing clinopyroxene and aluminous spinel, the harzburgites probably equilibrated at pressures higher than 1 GPa and lower than ~2 GPa (e.g., [22,23]). With an average temperature of 850°C, and an assumed pressure of 1.5 GPa, this places the Wiedemann harzburgites at temperatures ~300–500°C higher than calculated Archaean shield geotherms (40 mW/m^2, e.g., [24]), and observed 'geotherms' preserved by garnet peridotite xenoliths from the Kaapvaal, Wyoming and Siberian cratons (e.g., [4,19,25]).

There are at least three possible interpretations of this data. Either the xenoliths equilibrated along a conductive geotherm in thin continental lithosphere, or they were heated above an Archaean cratonic geotherm during Tertiary rifting and the passage of the Iceland mantle plume beneath this region, or 850°C is a closure temperature unrelated to the geotherm. The temperature of 850°C at 1.5 GPa is similar to those for spinel–peridotite xenoliths from the extensional environment at Baja California [26], and lower by ~100°C than those for peridotites associated with continental flood basalts from eastern China and Australia [27,28].

Three possible ages and processes for the genesis of the Wiedemann harzburgites can be envisioned: (1) an Archaean origin, possibly linked to the generation of the ~3 Ga central Greenland craton; (2) formation during the Caledonian orogeny, known to have affected the Greenland crust extensively to the north [16]; (3) lithospheric, depleted mantle formed during Tertiary magmatism and rifting.

For origin (3), the harzburgite would have had to cool to the average equilibrium temperature of 850°C in less than 15 Ma, which is the maximum time interval between the main basaltic melt production along the continental margin and the emplacement of the xenolith-bearing dykes (see above). With an initial temperature of 1300°C or more at the time of emplacement of the harzburgite at 45 km depth, the time needed for cooling to 850°C is ~40 Ma or more following the initiation of conductive heat transfer, given an average thermal diffusivity for the lithosphere of 1×10^{-6} m^2/s (e.g., [29]). To reach ~850°C in 15 Ma, the overlying lithosphere would have to be 30 km thick or less, which appears unlikely. Although a Tertiary origin for these xenoliths cannot completely be ruled out, the most likely origin of the Wiedemann harzburgites is either: (1) within the lithospheric mantle with comparable age to the overlying Archaean craton; or (2) beneath a subduction-related magmatic system at some time prior to the end of the Caledonian orogeny. These possibilities will be reviewed below.

5.2. Comparison to other mantle peridotites

The harzburgite xenoliths from Wiedemann Fjord have Fo in olivine among the highest known in mantle peridotite samples, only paralleled by some xenoliths from Archaean cratons, mainly the Kaapvaal province, and by the poorly known Papuan Ultramafic Belt. Further, the Wiedemann xenoliths have a unique composition because of their high modal olivine contents (Fig. 6). This places the Wiedemann xenoliths outside the field defined by xenoliths from Archaean cratons as well as from younger continental areas [3]. Compared to worldwide occurrences of spinel and garnet lherzolites and harzburgites (Fig. 7, [30]) the Wiedemann xenoliths are highly depleted in CaO and Al_2O_3, and are at the lower end of the SiO_2 range. In terms of MgO, the Wiedemann xenoliths lie along and above the upper limit of previous xenolith data, while in terms of

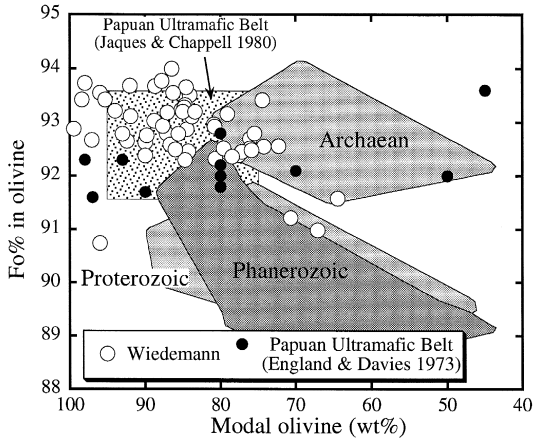

Fig. 6. Forsterite (Fo) in olivine versus the modal olivine content for individual samples. The fields of Archaean, Proterozoic, and Phanerozoic represent the compositional fields of mantle peridotite xenoliths from continental crustal areas of the given age [3]. Box gives the range of compositions reported for Papuan mantle tectonites [86].

FeO, they are similar to garnet peridotites, but have less FeO than any reported spinel peridotites.

Compared to peridotites from oceanic settings, the Wiedemann xenoliths have higher Fo in olivine, higher modal olivine, and lower whole-rock Al_2O_3 and CaO (e.g., [31]). Subduction-related peridotites from oceanic trenches and the South West Pacific ophiolites have olivine as high as Fo_{92}, but all are less than $Fo_{92.5}$ (Fig. 4d).

The refractory nature of many mantle-derived peridotites has long been interpreted as the result of melt extraction. Fo in olivine and Cr# of spinel in the residue correlate positively with degree of melting (e.g., [32]). Since chromian spinel is a common phase in peridotites of mantle origin, and exhibits a large compositional variation, it has been widely used to evaluate the genesis of the host rock (e.g., [20,32–34]). In Fig. 4a, the Wiedemann spinels are compared to spinels from depleted spinel peridotite xenoliths (garnet-free) from the Kaapvaal, Wyoming, and Siberian cratons. Cratonic xenolith spinels cover the same large range in Cr# as the Wiedemann spinels; all be classified as alpine peridotites Type II, based on their Cr# alone [33]. Whereas the origin of the sub-cratonic xenoliths is debated, the Type II alpine peridotites are thought to form within subduction-related magmatic arcs, where the apparent high degrees of melting (high Cr# and Fo in spinel and olivine, respectively) may be related to remelting of residual oceanic peridotites due to introduction of H_2O into the mantle source from the subducting slab [33,35].

Spinels from arc-related peridotites have lower Mg# at a given Cr# than spinels from cratonic peridotites, as demonstrated by spinels from Japanese peridotite massifs, Tonga and Marianas fore-arc regions, and from the New Caledonia and Papua New Guinea ophiolites (Fig. 4c). These may all be residues of hydrous melting of upper mantle in an island arc environment, and their lower Mg# in spinels could be due to relatively low temperature equilibration [33], or to relatively high oxygen fugacity which produces a pyroxene + magnetite component in spinel at the expense of olivine.

Arai [20,34] combined Fo and Cr# in co-existing olivine–spinel assemblages to distinguish between residual mantle peridotites from different environments. The available data for arc-related peridotite

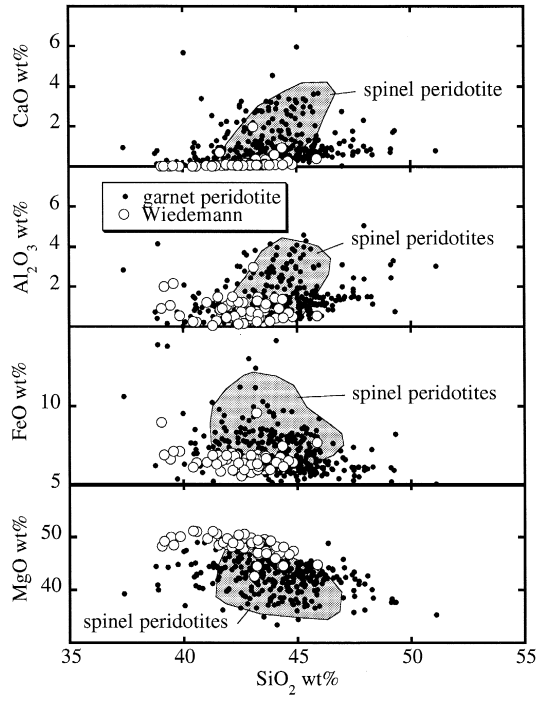

Fig. 7. Major elemental variation in Wiedemann xenoliths compared to the overall variation of peridotites of presumed mantle origin, compiled by McDonough and Frey [30]. In general, the Wiedemann harzburgites are lower in SiO_2, CaO, Al_2O_3 and FeO and higher in MgO relative to the bulk of the compiled peridotite xenoliths.

massifs and abyssal peridotites largely plot within the center of the 'olivine–spinel mantle array' (OSMA), while the Wiedemann xenoliths and other cratonic spinel peridotites generally define the low spinel Cr#/high Fo edge of OSMA (Fig. 4b,d). One way to interpret the relatively low spinel Cr# at a given Fo content for sub-cratonic peridotites is that the Cr# of spinel in a given peridotite assemblage decreases with increasing pressure of equilibration [20,33,36]. Also, if residual garnet is present, later metamorphic breakdown of garnet will produce spinel with a relatively low Cr. Thus, low spinel Cr#/Fo in cratonic xenoliths, and specifically in the Wiedemann harzburgites, reflect melting events at relatively high pressures compared to abyssal and arc peridotites. This is not surprising, as the abyssal and arc peridotites that can be sampled at the Earth's surface underwent decompression melting nearly to the base of thin, oceanic crust.

5.3. Possible relation to arc petrogenesis

The similarities between harzburgites from Wiedemann, and those from ophiolites of Papua New Guinea (PNG) and New Caledonia (NC) in terms of modal olivine and Fo contents (Fig. 6) may suggest a genetic link. Therefore, one hypothesis is that the Wiedemann harzburgites, along with PNG and NC harzburgites, formed via reaction between ascending melt and upper mantle peridotite, involving dissolution of pyroxene from previously depleted peridotites (e.g., [37]). Increasing magma mass during such reaction under isothermal, isenthalpic or adiabatic conditions [37,38] would lead to increasing Mg# in the residues compared to the protolith. If the melt/rock reaction process occurred in the overthrust plate of a subduction zone, the Wiedemann harzburgites would have formed in a deeper portion of the mantle wedge compared to the PNG + NC suites, following the discussion of the spinel Cr#/olivine Fo relationship in the preceding section of this paper.

It is apparent that dissolution of pyroxene in migrating melt would produce a derivative liquid with higher SiO_2 than the initial liquid. This is consistent with the fact that Phanerozoic magmas with high Cr# spinel and high Fo olivine are virtually all arc-related, and are commonly boninites and high Mg# andesites (e.g., [39] and compilations in [20,33,36]). Furthermore, the few trace element analyses of NC peridotites suggest a role for melt/rock reaction in their origin [40,41]. However, this hypothesis is difficult to constrain more fully at present due to uncertainties regarding the composition of liquid reactants and products, and the relative lack of data on PNG peridotites.

5.4. Possible relation to komatiite genesis

Table 1 lists two hypothetical, primitive mantle compositions, pyrolite [42] and Hart and Zindler's primitive upper mantle (PUM, [43]), that span the range of all proposed primitive mantle compositions. Using simple mass balance (source = residue + melt), the average composition of Wiedemann harzburgite xenoliths was subtracted from primitive upper mantle to give a resulting melt composition that is in equilibrium with the average olivine in the xenoliths ($Fo_{92.7}$), using the olivine/liquid Fe/Mg Kd of Ulmer [44] at 2 GPa. This yields an estimated degree of melting of 40 wt% using pyrolite, and 38 wt% using PUM. Note that, assuming melting occurred in a single episode with these source mantle compositions, this calculation is independent of the melting process (e.g., batch, fractional, etc.), and yields the composition of the aggregate liquid extracted.

The value of $\sim$40% melting for the generation of harzburgite xenoliths with olivine $\sim Fo_{92.7}$ is in accordance with several melting experiments. For example, residues of melting of Kettle River peridotite (very close to pyrolite) reach $Fo_{92.1-92.2}$ between 35% and 37% melting at 3, 4 and 5 GPa, $Fo_{92.5-92.6}$ between 35% and 41% melting at 6 and 7 GPa, and $Fo_{93.0}$ at 52% melting at 3 GPa [45].

The very low modal contents of clinopyroxene ($< 1\%$) in Wiedemann xenoliths with olivine $> Fo_{92}$ suggest that the xenoliths reached clinopyroxene-out during partial melting. The clinopyroxene now present in the harzburgites may represent crystallized, retained melt. Experimental melting of primitive peridotite shows that calcic clinopyroxene is exhausted at $\sim$20–30% melting in the pressure range 1.5–4 GPa, depending on starting composition and pressure of melting [45–48].

The highly forsteritic olivine and low modal orthopyroxene in the average Wiedemann harzburgite further suggest that the hypothetical melting event

took place well within the four-phase liquid–orthopyroxene–olivine–chrome spinel field, possibly approaching orthopyroxene-out. The degree of melting at which all pyroxene becomes exhausted appears to be relatively insensitive to pressure, and is 40–45% at 1.5 GPa [46], and roughly bracketed between 35% and 52% at 3–7 GPa [45,47]. However, note that the experimental data here cited are for nominally anhydrous systems. Because the addition of H_2O increases the size of the olivine primary phase volume, the resulting liquid would have more SiO_2 and pyroxene would be exhausted at smaller degrees of melting under hydrous conditions.

The calculated melts extracted from primitive mantle to produce average Wiedemann harzburgite (Table 1) have SiO_2 contents between 48.8 wt% and 51.4 wt%, and MgO between 22.6 wt% and 20.4 wt%, using pyrolite and PUM, respectively. Such compositions are typical of high degree melts at moderate pressures (2–3 GPa) as demonstrated by the experimental data of [49] and [45] (Fig. 8 and Table 1). For experimental melts with appropriate Mg#, SiO_2 varies between 48 wt% and 50 wt%, and MgO varies between 20 wt% and 25 wt%. These experimental melts were produced from primitive mantle peridotite compositions, and coexist with a harzburgitic or dunitic residue with between $Fo_{92.1}$ and $Fo_{93.6}$, the same as the compositional range of olivine from the Wiedemann harzburgites. Fig. 8 demonstrates that the pyrolite-based, calculated melt for average Wiedemann harzburgite is close to the experimental melts in terms of SiO_2, MgO, FeO, CaO and Al_2O_3. Thus, the composition of the average Wiedemann harzburgite is broadly consistent with the extraction of $\sim$40% melt at moderate pressure.

Such high degrees of melting have been proposed for the generation of komatiites [50,51]. Komatiites largely fall in two groups, the Barberton and Munro-types [52]. Due to their high MgO contents and low concentrations of SiO_2, CaO, Al_2O_3 and incompatible elements, relative to, for example, present mid-ocean ridge basalts, it has been proposed that komatiites were generated by high degrees of melting ($>$ 30%) at high pressures ($>$ 7 GPa for Barberton-types, and 9–5 GPa for Munro-types) [45,53–57].

Munro-type komatiites, particularly occurring in the late Archaean, have higher SiO_2 than Barberton-types, and have CaO/Al_2O_3 weight ratios close to primitive mantle ($\sim$ 1.0). Compositions for Munro-type komatiites are also presented in Fig. 8, selected using the 'olivine control line' criterion described by [52] to avoid samples that may have experienced loss or gain of major elements during metamorphism and alteration, and restricted to Mg# of 78–82 (equilibrium olivine $Fo_{92-93.5}$ at 2 GPa). The resulting Munro komatiite field lies close to the pyrolite-based, calculated melt for Wiedemann, and close to the 36–52% experimental melts at 2–3 GPa.

We first note that Munro-type komatiites may have been produced by extensive melting at average pressures of $\sim$2–3 GPa. However, the Munro-type komatiite field differs slightly, but consistently, from calculated and experimental melts, having lower SiO_2 and Al_2O_3, and higher FeO. Increasing pressure results in increasing FeO and MgO and decreasing SiO_2 in partial melts of mantle peridotite (e.g., [58]). For example, Walter [45] reports an 11% partial melt of primitive peridotite at 6 GPa with low SiO_2 (44.97 wt%) and high FeO (12.64 wt%) (Fig. 8). Munro-type komatiites plot between this 6 GPa melt and the experimental 2–3 GPa melts.

The experiments of Falloon et al. [49] and Walter [45] closely approximate isobaric batch melting, in contrast to current models of polybaric, near-fractional mantle melting (e.g., [59,60]). Similar, polybaric melting hypotheses have recently been proposed for komatiites [57,61]. The compositions of the Munro-type komatiites may be produced by such a polybaric melting process, with melting initiated at roughly 7 GPa, and extending to 2–3 GPa or less, accompanied by aggregation of partial melts.

If the Wiedemann harzburgites are among the shallowest residues of a polybaric, near-fractional melting process, they would be in equilibrium with the last extracted melts, which could explain the lower FeO and SiO_2 in calculated extracted liquids compared to Munro-type komatiites. Since the degrees of melting inferred for the generation of the Wiedemann harzburgites proceeds beyond clinopyroxene- and garnet-out, Al_2O_3 and CaO in the calculated extracted melts is little fractionated relative to primitive mantle compositions, with a weight ratio of CaO/Al_2O_3 around unity. The pyrolite-based, calculated melt has a CaO/Al_2O_3 ratio of 1.06, typical of the Munro-type komatiites that have ratios ranging

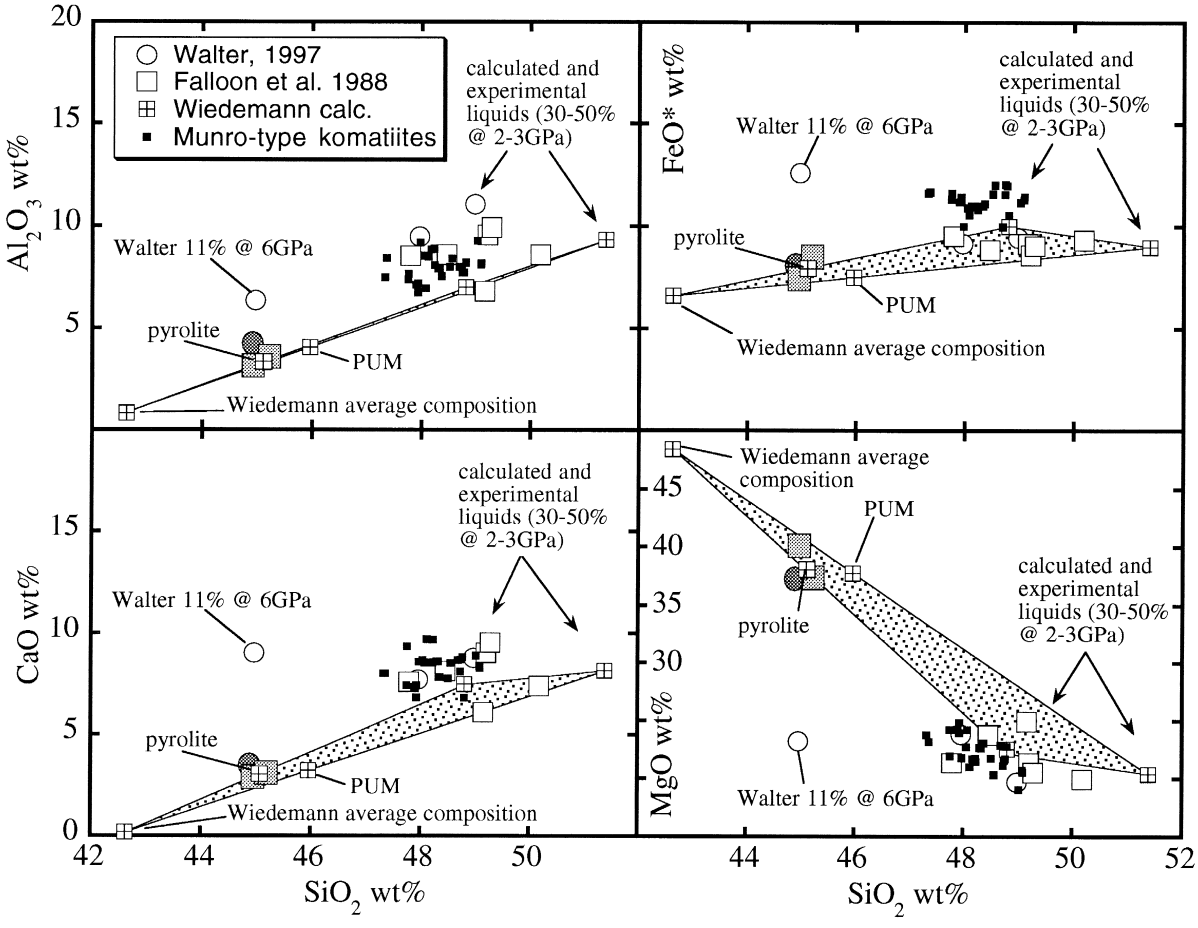

Fig. 8. The major element composition of the average Wiedemann harzburgite, calculated on the basis of all samples and of the calculated extracted melts (crossed boxes) using pyrolite and PUM as primitive mantle compositions (see text and Table 1 — compositions with tie lines). The compositions of the starting material for experimental melting studies by Falloon et al. [49] (filled boxes) and Walter [45] (dot) are also shown. The corresponding high-degree melt compositions are plotted using the same symbols as for the starting compositions. An experimental melt at moderate melting degree (11%) and high pressure (6 GPa) given by Walter [45] is also plotted. Black boxes are Munro-type komatiites (Herzberg, pers. commun., 1997, and Belingwe [87]; Kambalda [54,88,89]). Note the similarity of the Wiedemann extracted melt, calculated using pyrolite as starting material, with experimental high degree melts at 2–3 GPa. Munro-type komatiites are similar in composition to both calculated and experimental melts, but are displaced slightly towards lower SiO_2 and higher FeO, as for smaller degree melts at higher pressure, as indicated by Walter's [45] 11% melt at 6 GPa.

from 0.9 to 1.2. Similarly, the rare earth element patterns of Munro-type komatiites are flat at about 1–2 times primitive mantle, consistent with 40% melting of primitive mantle leaving a harzburgitic residue.

One of the main problems in linking depleted peridotite xenoliths to the generation of komatiites has been that many cratonic mantle xenoliths with high Fo olivine, candidates for being the residues of komatiite extraction, also have >31 wt% orthopyroxene (e.g., Kaapvaal peridotites, [7]). These xenoliths are too rich in silica to be simply related to the extraction of komatiites from primitive mantle compositions [7,62,63]. Instead, it has been suggested that the orthopyroxene-rich harzburgites formed by metamorphic differentiation of a lower SiO_2 protolith [7], as cumulates from ultramafic melts [57,63], or as a product of reaction between an already

depleted, olivine-rich harzburgite protolith and ascending melts, with either basaltic [62] or silicic compositions [64–67].

The Wiedemann harzburgites have SiO_2 lower than the average peridotite from the Kaapvaal province (average 42.61 wt% versus 44–49 wt%, respectively). As stated above, the Wiedemann harzburgites could be residues after extraction of high-degree melts, resembling Munro-type komatiites. This viewpoint may find further support in the scarcity of hydrous phases in the Weidemann xenoliths. Many mantle xenoliths from other cratonic areas have undergone fluid- and/or melt–rock reactions that have modified the chemical composition of the rock (e.g., [68–70]). Since the metasomatic agents arise in underlying asthenospheric mantle or subduction, the domain most likely to have retained its pristine residual composition would reside in the uppermost mantle, where it would be 'shielded' from migrating metasomatic fronts [3].

Acknowledgements

We thank John Fløng and Jørn Rønsbo for assistance at the microprobe facility at the Geological Institute, University of Copenhagen. Göran Lindmark is thanked for his fine helicopter handling. Our 1995 field season was coordinated by the indefatigable Troels F.D. Nielsen and was supported by the Danish Lithosphere Centre (DLC) and the Woods Hole Oceanographic Institution. Joe Boyd, Claude Herzberg and Mike Walter generously provided unpublished data and preprints. Constructive criticism by Lotte M. Larsen, Troels F.D. Nielsen, Ole Stecher and Peter Thy, along with reviews by Claude Herzberg, Nick Arndt and two anonymous reviewers, are greatly appreciated. Sample analysis and preparation of this paper were supported by the DLC and NSF Research Grant OCE-9416631. *[FA]*

References

[1] P.H. Nixon, F.R. Boyd, Petrogenesis of the granular and sheared ultrabasic nodule suite in kimberlites, in: P.H. Nixon (Ed.), Lesotho Kimberlites, Lesotho National Development Corporation, Maseru, Lesotho, 1973, pp. 48–56.

[2] B. Harte, Mantle peridotites and processes, the kimberlite sample, in: C.J. Hawkesworth, M.J. Norry (Eds.), Continental Basalts and Mantle Xenoliths, Shiva, Nantwich, UK, 1983, pp. 46–91.

[3] M.A. Menzies, Archaean, Proterozoic, and Phanerozoic lithosphere, in: M.A. Menzies (Ed.), Continental Mantle, Oxford University Press, Oxford, 1990, pp. 67–86.

[4] F.R. Boyd, N.P. Pokhilenko, D.G. Pearson, S.A. Mertzman, N.V. Sobolev, L.W. Finger, Composition of the Siberian cratonic mantle: Evidence from Udachnaya peridotite xenoliths, Contrib. Mineral. Petrol., in press.

[5] M.J. O'Hara, M.J. Saunders, E.L.P. Mercy, Garnet–peridotite, primary ultrabasic magma and eclogite; Interpretation of upper mantle processes in kimberlite, Phys. Chem. Earth 9 (1975) 571–604.

[6] T.H. Jordan, Mineralogies, densities and seismic velocities of garnet lherzolites and their geophysical implications, in: The mantle sample: Inclusions in kimberlites and other volcanics, F.R. Boyd, H.O.A. Meyer, Eds., pp. 1–14, AGU, Washington, D.C., 1979.

[7] F.R. Boyd, Compositional distinction between oceanic and cratonic lithosphere, Earth Planet. Sci. Lett. 96 (1989) 15–26.

[8] F.R. Boyd, S.A. Mertzman, Composition and structure of the Kaapvaal lithosphere, southern Africa, in: Magmatic processes: Physiochemical Principles, B.A. Mysen, Ed. Special Publication 1, pp. 13–24, The Geochemical Society, University Park, PA, 1987.

[9] C.K. Brooks, J.C. Rucklidge, A Tertiary lamprophyre dike with high pressure xenoliths and megacrysts from Wiedemanns Fjord, East Greenland, Contrib. Mineral. Petrol. 42 (1973) 197–212.

[10] L.R. Wager, Geological investigations in East Greenland Part I. General geology from Angmagssalik to Kap Dalton, Meddr. Grønland 105 (2) (1934) 46.

[11] H. Hansen, D.C. Rex, P.G. Guise, C.K. Brooks, 40Ar/39Ar ages on early Tertiary basalts from the Scoresby Sund area, East Greenland, Newslett. Strat. 32 (1995) 103–116.

[12] M. Storey, R.A. Duncan, H.C. Larsen, R. Waagstein, L.M. Larsen, C. Tegner, C.E. Lesher, Impact and Rapid flow of the Iceland plume beneath Greenland at 61 Ma, EOS Trans. Am. Geophys. Union 77 (1996) F839.

[13] A.K. Pedersen, M. Watt, W.S. Watt, L.M. Larsen, Structure and stratigraphy of the Early Tertiary basalts of the Blosseville Kyst, East Greenland, J. Geol. Soc. Lond. 154 (1997) 565–570.

[14] C. Tegner, S. Bernstein, D.K. Bird, R.A. Duncan, M. Storey, C.K. Brooks, H.C. Larsen, Age and emplacement history of East Greenland gabbro intrusions, EOS Trans. Am. Geophys. Union 77 (46) (1996) F845.

[15] P.N. Taylor, F. Kalsbeek, D. Bridgwater, Discrepancies between neodymium, lead and strontium model ages from the Precambrian of southern East Greenland: Evidence for a Proterozoic granulite-facies event affecting Archaean gneisses, Chem. Geol. 94 (1992) 281–291.

[16] N. Henriksen, The Caledonides of central East Greenland 70°–76°N, in: The Caledonides Orogen—Scandinavia and Related Areas, D.G. Gee, B.A. Sturt, Eds., pp. 1095–1113, 1985.

[17] B. Harte, Rock nomenclature with particular relation to deformation and recrystallization textures in olivine-bearing xenoliths, J. Geol. 85 (1977) 279–288.
[18] F. Kalsbeek, Note on the reliability of point counter analyses, Neues Jahrb. Mineral., Monatsh. 1 (1969) 1–6.
[19] G.P. Brey, T. Kšhler, Geothermobarometry in four-phase lherzolites II. New thermobarometers, and the practical assessment of existing thermobarometers, J. Petrol. 31 (6) (1990) 1353–1378.
[20] S. Arai, Characterization of spinel peridotites by olivine–spinel compositional relationships: Review and interpretation, Chem. Geol. 113 (1994) 191–204.
[21] G. Witt-Eickschen, H.A. Seck, Solubility of Ca and Al in orthopyroxene from spinel peridotite: An improved version of an empirical geothermometer, Contrib. Mineral. Petrol. 106 (1991) 431–439.
[22] D.H. Green, W. Hibberson, The instability of plagioclase in peridotite at high pressure, Lithos 3 (1970) 209–221.
[23] H.S.C. O'Neill, The transition between spinel lherzolite and garnet lherzolite, and its use as a geobarometer, Contrib. Mineral. Petrol. 77 (1981) 185–194.
[24] D.H. Green, A.E. Ringwood, The genesis of basaltic magmas, Contrib. Mineral. Petrol. 15 (1967) 103–190.
[25] A.A. Finnerty, F.R. Boyd, Thermobarometry for garnet peridotites: Basis for the determination of thermal and compositional structure of the upper mantle, in: Mantle xenoliths, P.H. Nixon, Ed., pp. 381–402, John Wiley and Sons, New York, 1987.
[26] N. Cabanes, J.-C.C. Mercier, Insight into the upper mantle beneath an active extensional zone: The spinel–peridotite xenoliths from San Quitin (Baja California Mexico),, Contrib. Mineral. Petrol. 100 (1988) 374–382.
[27] X. Xu, S.Y. O'Reilly, X. Zhou, W.L. Griffin, A xenolith-derived geotherm and the crust-mantle boundary at Qilin, southeastern China, Lithos 38 (1996) 41–62.
[28] S.Y. O'Reilly, W.L. Griffin, A xenolith-derived geotherm for southeastern Australia and its geophysical implications, Tectonophysics 111 (1985) 41–63.
[29] D.L. Turcotte, G. Schubert, Geodynamics — application of continuum physics to geological problems, 450 pp., John Wiley and Sons, New York, 1982.
[30] W.F. McDonough, F.A. Frey, Rare Earth Elements in Upper Mantle Rocks, in: Geochemistry and Mineralogy of Rare Earth Elements, B.R.L.G.A. McKay, Ed., 21, pp. 99–145, The Mineralogical Society of America, Washington, D. C., 1989.
[31] E. Bonatti, P.J. Michael, Mantle peridotites from continental rifts to ocean basins to subduction zones, Earth Planet. Sci. Lett. 91 (1989) 297–311.
[32] T.N. Irvine, Chromian Spinel as a petrogenetic indicator, Can. J. Earth Sci. 2 (1965) 648–672.
[33] H.J.B. Dick, T. Bullen, Chromian spinel as a petrogenetic indicator in abyssal and alpine-type peridotites and spatially associated lavas, Contrib. Mineral. Petrol. 86 (1984) 54–76.
[34] S. Arai, An estimation of the least depleted spinel peridotite on the basis of olivine–spinel mantle array, Neues Jahrb. Mineral., Monatsh. H8 (1987) 347–354.
[35] A. Miyashiro, The Troodos ophiolitic complex was probably formed in an island arc, Earth Planet. Sci. Lett. 19 (1973) 218–224.
[36] A.V. Sobolev, L.V. Danyushevsky, Petrology and geochemistry of boninites from the north termination of the Tonga Trench: constraints on the generation conditions of primary high-Ca boninite magmas, J. Petrol. 35 (1994) 1183–1211.
[37] P.B. Kelemen, Reaction between ultramafic rock and fractionating basaltic magma I. Phase relations, the origin of calc-alkaline magma series, and the formation of discordant dunite, J. Petrol. 31 (1) (1990) 51–98.
[38] P.B. Kelemen, J.A. Whitehead, E. Aharonov, K.A. Jordahl, Experiments on flow focusing in soluble porous media, with application to melt extraction from the mantle, J. Geophys. Res. 100 (B1) (1995) 475–496.
[39] Y. Tatsumi, K. Ishizaka, Existence of andesitic primary magma: An example from southwest Japan, Earth Planet. Sci. Lett. 53 (1981) 124–130.
[40] A. Prinzhofer, C.J. Allegre, Residual peridotites and the mechanisms of partial melting, Earth Planet. Sci. Lett. 74 (1985) 251–265.
[41] O. Navon, E. Stolper, Geochemical consequences of melt percolation: The upper mantle as a chromatographic column, J. Geol. 95 (1987) 285–307.
[42] A.E. Ringwood, The chemical composition and the origin of the Earth, in: Advances in Earth Science, P. Hurley, Ed., pp. 287–356, 1966.
[43] S.R. Hart, A. Zindler, In search of a bulk-earth composition, Chem. Geol. 57 (1986) 247–267.
[44] P. Ulmer, The dependence of the Fe^{2+}–Mg cation-partitioning between olivine and basaltic liquid on pressure, temperature and composition, Contrib. Mineral. Petrol. 101 (1989) 261–273.
[45] M.J. Walter, Melting of garnet peridotite and the origin of komatiite and depleted lithosphere, J. Petrol. in press, 1997.
[46] E. Takahashi, T. Shimazaki, Y. Tsuzaki, H. Yoshida, Melting study of a peridotite KLB-1 to 6.5 GPa, and the origin of basaltic magmas, in: Melting and melt movement in the Earth, K.G. Cox, D. McKenzie, R.S. White, Eds. A 342, pp. 105–120, Oxford University Press, Oxford, 1993.
[47] C. Herzberg, Depth and degree of melting of komatiites, J. Geophys. Res. 97 (1992) 4521–4540.
[48] K. Hirose, I. Kushiro, Partial melting of dry peridotites at high pressures: Determination of compositions of melts segregated from peridotite using aggregates of diamond, Earth Planet. Sci. Lett. 114 (1993) 477–489.
[49] T.J. Falloon, D.H. Green, C.J. Hatton, K.L. Harris, Anhydrous partial melting of a fertile and depleted peridotite from 2 to 30 kb and application to basalt petrogenesis, J. Petrol. 29 (6) (1988) 1257–1282.
[50] M.J. Viljoen, R.P. Viljoen, Evidence for the existence of a mobile extrusive peridotitic magma from the Komati Formation of the Onverwacht Group, Geol. Soc. South Africa Spec. Pub. 2 (1969) 87–112.
[51] D.H. Green, Archean greenstone belts may include terrestrial equivalents of lunar maria?, Earth Planet. Sci. Lett. 15 (1972) 263–270.

[52] N.T. Arndt, Archean komatiites, in: Archean crustal evolution, K.C. Condie, Ed. Developments in Precambrian geology, 11, pp. 11–44, Elsevier, Amsterdam, 1994.
[53] E. Takahashi, Speculations on the Archean mantle: Missing link between komatiite and depleted garnet peridotite, J. Geophys. Res. 95 (1990) 15941–15954.
[54] N.T. Arndt, C.M. Lesher, Fractionation of REE by olivine and the origin of Kambalda komatiites, Western Australia, Geochim. Cosmochim. Acta 56 (1992) 4191–4204.
[55] E.G. Nisbet, M.J. Cheadle, N.T. Arndt, M.J. Bickle, Constraining the potential temperature of the Archaean mantle: A review of the evidence from komatiites, Lithos 30 (1993) 291–307.
[56] C. Herzberg, Generation of plume magmas through time: An experimental perspective, Chem. Geol. 126 (1995) 1–16.
[57] C. Herzberg, Phase equilibrium constraints on the origin of basalts, picrites, and komatiites, Earth-Sci. Rev. in press, 1997.
[58] M.J. O'Hara, Primary magmas and the origin of basalts, Scot. J. Geol. 1 (1965) 19–40.
[59] C.H. Langmuir, J.F. Bender, A.E. Bence, G.N. Hanson, S.R. Taylor, Petrogenesis of basalts from the Famous area, Mid-Atlantic Ridge, Earth Planet. Sci. Lett. 36 (1977) 133–156.
[60] D. McKenzie, The generation and compaction of partially molten rock, J. Petrol. 25 (1984) 713–765.
[61] N.T. Arndt, A.C. Kerr, J. Tarney, Dynamic melting in plume heads: The formation of Gorgona komatiites and basalts, Earth Planet. Sci. Lett. in press, 1997.
[62] P.B. Kelemen, H.J.B. Dick, J.E. Quick, Formation of harzburgite by pervasive melt/rock reaction in the upper mantle, Nature 358 (1992) 635–641.
[63] C.T. Herzberg, Lithosphere peridotites of the Kaapvaal Craton, Earth Planet. Sci. Lett. 120 (1993) 13–29.
[64] A.E. Ringwood, The petrological evolution of island arc systems, J. Geol. Soc. London 130 (1974) 183–204.
[65] R.L. Rudnick, W.F. McDonough, A. Orpin, Northern Tanzanian peridotite xenoliths: a comparison with Kaapvaal peridotites and inferences on metasomatic interactions, in: Kimberlites, related rocks and mantle xenoliths, H.O.A. Meyer, O. Leonardos, Eds. 1, pp. 336–353, CPRM, Brasilia, Brazil, 1994.
[66] P.B. Kelemen, N. Shimizu, T. Dunn, Relative depletion of niobium in some arc magmas and the continental crust: Partitioning of K, Nb, La and Ce during melt/rock reaction in the upper mantle, Earth Planet. Sci. Lett. 120 (1993) 111–134.
[67] P.B. Kelemen, S.R. Hart, Silica enrichment in the continental lithosphere via melt/rock reaction, J. of Conf. Abstr. (Goldschmidt Conference) 1 (1996) 308.
[68] M. Menzies, A. Halliday, Lithospheric mantle domains beneath the Archean and Proterozoic crust of Scotland, J. Petrol. (Special Lithosphere Issue), 275–302, 1988.
[69] Y. Liang, D. Elthon, Geochemistry and petrology of spinel lherzolite xenoliths from Xalapasco de La Joya, San Luis Potosi, Mexico: Partial Melting and Mantle Metasomatism, J. Geophys. Res. 95 (1990) 15859–15877.
[70] S.E. Kesson, A.E. Ringwood, Slab–mantle interactions 1. Sheared and refertilised garnet peridotite xenoliths — Samples of Wadati–Benioff zones?, Chem. Geol. 78 (1989) 83–96.
[71] D.A. Carswell, D.B. Clarke, R.H. Mitchell, The petrology and geochemistry of ultramafic nodules from Pipe 200, northern Lesotho, in: The mantle sample: Inclusions in kimberlites and other volcanics, F.R. Boyd, H.O.A. Meyer, Eds., pp. 127–144, AGU, Washington, D.C., 1979.
[72] I.D. MacGregor, Mafic and ultramafic xenoliths from the Kao kimberlite pipe, in: The mantle sample: Inclusions in kimberlites and other volcanics, F.R. Boyd, H.O.A. Meyer, Eds., pp. 156–172, AGU, Washington, D. C., 1979.
[73] R.L. Hervig, J.V. Smith, I.M. Steele, J.B. Dawson, Fertile and barren Al–Cr-spinel harzburgites from the upper mantle: Ion and electron probe analyses of trace elements in olivine and orthopyroxene: relation to lherzolites, Earth Planet. Sci. Lett. 50 (1980) 41–58.
[74] D.H. Eggler, M.E. McCallum, M.B. Kirkly, Kimberlite-transported nodules from Colorado—Wyoming; A record of enrichment of shallow portions of an infertile lithosphere, Geol. Soc. America Spec. Pap. 215 (1987) 77–90.
[75] G. Chazot, M.A. Menzies, B. Harte, Determination of partition coefficients between apatite, clinopyroxene, amphibole, and melt in natural spinel lherzolites from Yemen: Implications for wet melting of the lithospheric mantle, Geochim. Cosmochim. Acta 60 (3) (1996) 423–437.
[76] N. Takahashi, Evolutional history of the uppermost mantle of an arc system: Petrology of the Horoman Peridotite Massif, Japan, in: Ophiolite genesis and evolution of the ocean lithosphere, T. Peters, A. Nicolas, R.G. Coleman, Eds., pp. 195–205, Kluwer Academic Publishers, Dordrecht, 1991.
[77] E. Takazawa, Geodynamic evolution of the Horoman peridotite, Japan: Geochemical study of lithospheric and asthenospheric processes, Ph.D., 562 p, MIT, 1996.
[78] K. Ozawa, Ultramafic tectonite of the Miyamori ophiolitic complex in the Kitakami Mountains, Northeast Japan: Hydrous upper mantle in an island arc, Contrib. Mineral. Petrol. 99 (1988) 159–175.
[79] K. Ozawa, Melting and melt segregation in the mantle wedge above a subduction zone: evidence from the chromite-bearing peridotites of the Miyamori Ophiolite Complex, Northeastern Japan, J. Petrol. 35 (3) (1994) 647–678.
[80] S. Umino, E. Yoshizawa, Petrology of ultramafic xenoliths from Kishyuku Lava, Fukue-jima, Southwest Japan, Contrib. Mineral. Petrol. 124 (1996) 154–166.
[81] S. Arai, Dunite–harzburgite–chromitite complexes as refractory residue in the Sangun–Yamaguchi Zone, western Japan, J. Petrol. 21 (1980) 141–165.
[82] A.L. Jaques, D.H. Green, Anhydrous melting of peridotite at 0–15 Kb pressure and the genesis of tholeiitic basalts, Contrib. Mineral. Petrol. 73 (1980) 287–310.
[83] J. Moutte, Le Massif de Tiebaghi, Nouvelle Caledonia, et ses gites de chromite, Ph. D., L'ecole Nationale Superieure des Mines de Paris, 1979.
[84] S.H. Bloomer, R.L. Fisher, Petrology and geochemistry of igneous rocks from the Tonga Trench — a nonaccreting plate boundary, J. Geol. 95 (1987) 469–495.

[85] S.H. Bloomer, J.W. Hawkins, Gabbroic and ultramafic rocks from the Mariana Trench: an island arc ophiolite, in: Tectonic and geologic evolution of the SE Asian Seas and Islands 27, pp. 234–316, Am. Geophys. Union, Monograph, 1983.
[86] A.L. Jaques, B.W. Chappell, Petrology and trace element geochemistry of the Papuan Ultramafic Belt, Contrib. Mineral. Petrol. 75 (1980) 55–70.
[87] E.G. Nisbet, M.J. Bickle, A. Martin, The mafic and ultramafic lavas of the Belingwe greenstone belt, Rhodesia, J. Petrol. 18 (1977) 521–566.
[88] N.T. Arndt, G.A. Jenner, Crustally contaminated komatiites and basalts from Kambalda, Western Australia, Chem. Geol. 56 (1986) 229–255.
[89] K.P. Jochum, N.T. Arndt, A.W. Hofmann, Nb–Th–La in komatiites and basalts: Constraints on komatiite petrogenesis and mantle evolution, Earth Planet. Sci. Lett. 107 (1991) 272–289.